

# Cross-vendor validation of liver magnetic resonance elastography

Suraj D. Serai,<sup>1</sup> Meng Yin,<sup>2</sup> Hui Wang,<sup>3</sup> Richard L. Ehman,<sup>2</sup> Daniel J. Podberesky<sup>1,4</sup>

<sup>1</sup>Department of Radiology, Cincinnati Children's Hospital Medical Center, Cincinnati, OH, USA

<sup>2</sup>Department of Radiology, Mayo Clinic, Rochester, MN, USA

<sup>3</sup>Philips Healthcare, Cleveland, OH, USA

<sup>4</sup>Department of Radiology, Nemours Children's Hospital, Orlando, FL, USA

## Abstract

**Purpose:** To evaluate and validate the reproducibility of MR Elastography (MRE)-derived liver stiffness values on two different MR vendor platforms performed on the same subject on the same day.

**Methods:** This investigation was approved by the hospital IRB. MRE exams were performed twice in identical fashion in eight volunteers and in five clinical patients on two different 1.5 T MR scanners—once on a Philips MR scanner and immediately afterward in back-to-back fashion on a General Electric MR scanner, or vice versa. All scan parameters were kept identical on the two platforms to the best extent possible. After the MRE magnitude and phase images were obtained, the data were converted into quantitative images displaying the stiffness of the liver parenchyma. Mean liver stiffness values between the two platforms were compared using interclass correlation with a  $p$  value  $<0.05$  considered statistically significant.

**Results:** Interclass correlation coefficient (ICC) value of 0.994 was obtained for 13 subjects with  $p$  value  $<0.001$  indicating a significantly positive correlation.

**Conclusion:** As MRE gains in acceptance and as its availability becomes more widespread, it is important to ascertain and confirm that liver stiffness values obtained on different MRE vendor platforms are consistent and reproducible. In this small pilot investigation, we demonstrate that liver stiffness measurement with MRE is reproducible and has very good consistency across two vendor platforms.

**Key words:** MRE—Liver elastography—MRE validation

Chronic liver disease is a leading cause of morbidity and mortality worldwide [1–3]. While there are many potential etiologies for liver disease, if untreated, they can all progress to hepatic fibrosis, and eventually cirrhosis [4, 5]. The detection and staging of fibrosis is an important part of the diagnosis, surveillance, and treatment of chronic liver disease. There is increasing evidence that the progression of liver fibrosis may be halted or even reversed in its early stages with appropriate treatment prior to disease progression to irreversible cirrhosis [6]. Hence, early diagnosis, follow-up, and therapeutic monitoring of fibrogenesis, the process of generation of new connective tissue in a diseased liver, is of great clinical importance.

Liver dysfunction is initially diagnosed and monitored using blood tests. However, elevated liver enzymes may not accurately predict the degree of hepatocellular injury or fibrosis [7], necessitating other means of following the progression of disease. Liver ultrasounds can be done to evaluate the appearance of the liver, bile ducts, and blood vessels, but ultrasound is operator-dependent and interpretation can be subjective. If the cause or extent of the liver disease is unclear, patients will require a liver biopsy.

Traditionally, liver biopsy has been considered the gold standard for diagnosing and staging liver fibrosis. However, liver biopsy has several disadvantages including the risk of complications (including life-threatening complications), relatively high cost, sampling of only a small portion of the liver, and relatively poor patient acceptance, especially in children [8–10]. Additionally, histopathologic interpretation of liver biopsy specimens is subject to significant inter- and intra-observer variability [11].

Alternative methods to assess liver stiffness, and thus fibrosis, such as MR elastography (MRE) are gaining acceptance in routine clinical practice. MRE is a non-invasive imaging technique that measures liver stiffness and thus provides a quantitative measure of fibrosis. MRE

calculates tissue stiffness by imaging the shear waves propagating within the parenchyma. The technique has been shown to accurately detect and stage hepatic fibrosis in adults and children [12–17]. MRE is currently approved by the Food and Drug Administration (FDA) for clinical use on three vendor platforms. As MRE gains in acceptance and as its availability becomes more widespread, it is important to ascertain and confirm that liver stiffness values obtained on different MRE vendor platforms are consistent and reproducible, as patients may move from one geographic location to another and obtain surveillance MRE exams on different magnets.

To our knowledge, a direct head-to-head comparison between MRE-derived liver stiffness on the same subject performed on the same day in consecutive fashion between two different MR vendor platforms has not been reported. The purpose of this pilot investigation was to evaluate and validate the reproducibility of MRE-derived liver stiffness values on two different MR vendor platforms performed on the same subject on the same day. We hypothesized that there would be no statistically significant difference between MRE-derived liver stiffness values between the two platforms.

## Materials and Methods

Eight healthy volunteers (age range 31–55 years; 4 males and 4 females) with no prior history of liver disease were recruited for the study with IRB approval, and informed consent was obtained. The purposes and procedures of our investigations were fully explained to all subjects, and the study was performed after obtaining informed consent. Five clinical patients (age range 10–21 year; 2 males and 3 females) with chronic liver disease were also included under a separate IRB-approved protocol with waiver of consent. The clinical indications in these five

patients were: nonalcoholic fatty liver disease (1), status-post Fontan procedure (3), and one patient with Wiskott–Aldrich syndrome. There were no technical problems with any of the study examinations.

MRE exams were performed twice in identical fashion on two different 1.5 T MR scanners at the same institution—once on a Philips MR scanner (Ingenia, Philips Healthcare, Best, Netherlands) equipped with a gradient system with a maximum amplitude of 45 mT/m and a 200 mT/m/msec slew rate using the anterior–posterior coil combination, and immediately afterward (no more than 30 min in between exams) in back-to-back fashion on a General Electric MR scanner (HDx, GE Healthcare, Waukesha, USA) equipped with a gradient system with a maximum amplitude of 33 mT/m and a 150 mT/m/msec slew rate using the 8-channel Cardiac–Torso coil, or vice versa. The subjects arrived after fasting for 2 h and did not eat or drink between the two MRE exams in order to avoid any postprandial hepatic blood flow change with time. MRE equipment consists of an active and a passive driver system. The active driver is kept in the MR equipment room and the passive driver, connected to the active driver in the equipment room with a hollow plastic tube by a wave-guide, is placed on the subject's abdomen just under the RF coil during imaging in the MRI scanner (Fig. 1). The active driver generates low-frequency (60 Hz) sound waves which are transferred to the liver via the passive driver. The length of the plastic tube was identical on both systems. Passive driver positioning was identical to the extent possible for the two examinations. To help reduce anxiety and sudden movements in pediatric patients, we performed a pre-scan simulation mimicking the vibration during scanning. This adjustment enabled more successful scanning during the actual MRE sequence. The image acquisition technique used has been previously described

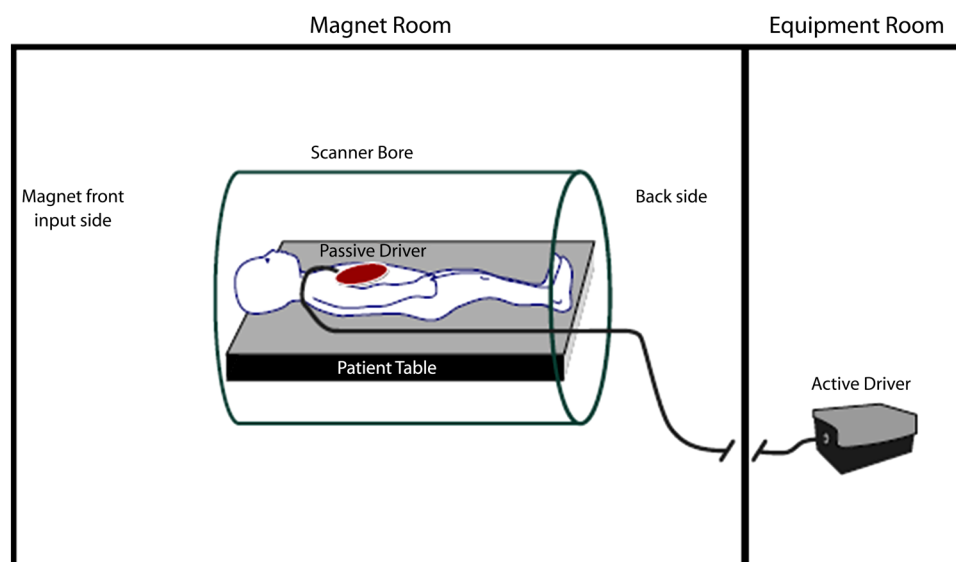


**Fig. 1.** A schematic diagram of subject set-up with the MRE hardware. The active driver is placed in the MR computer room and the passive driver, connected via a plastic tube through a wave-guide, is positioned over the liver region.

**Table 1.** MRE scan parameters

Sequence	Plane	TR (msec)	TE (msec)	Flip angle	Matrix size	Slice thickness (mm)	No. of averages
MRE	Axial	50	27	30	256 × 64	10	1

in detail [14]. The initiation and cessation of the low-frequency vibrations are controlled by the MR pulse sequence programmed and embedded as part of the scanner software. The MRE pulse sequence does not bypass any scanner safety standards as specified by the manufacturer. Four axial slices through the broadest portion of the liver were obtained for generation of shear wave images during breath-holds. All scan parameters were kept identical on the two platforms to the best extent possible. MRE MR parameters are shown in Table 1. MRE scan duration was identical on both platforms (~1 min), and data were acquired in four breath-holds of ~15 s each. After the MRE magnitude and phase images were obtained, the data were converted into elastograms using a direct inversion algorithm as described previously [18]. Post-processing of the images displaying the stiffness of the liver parenchyma is performed using MRE Wave software (Mayo Clinic, Rochester, MN) as an off-line post-processing tool. Stiffness values were obtained by drawing regions of interest (ROIs) around the entire liver on each axial slice, and a mean liver stiffness was then calculated from the four individual axial slice stiffness values. The ROIs were drawn by the same experienced observer in blinded fashion. Special care was taken to exclude large vessels and the central biliary tree when drawing the ROI. Mean liver stiffness values between the two platforms were compared using interclass correlation in Statistical Package for Social Sciences (SPSS) two-way mixed model with a  $p$  value  $<0.05$  considered statistically significant. Excellent agreement is considered when the interclass correlation coefficient (ICC) is greater than 0.85 [19, 20]. Bland–Altman difference plots were generated to assess the agreement between stiffness values obtained from both platforms. Scatter plot was generated to display the 95% prediction limits for the two datasets. A post hoc power analysis was performed on the combined dataset including all 13 subjects to determine the adequacy of the proposed sample size to detect the correlation of liver stiffness values between the two platforms.

## Results

Figure 2 shows a set of representative magnitude images, wave images, and stiffness maps from one of the subjects—top row shows GE scanner images and bottom row shows Philips scanner images. Mean liver stiffness values for the 8 volunteer subjects ranged from 1.96 to 2.65 kPa on the GE platform, and from 1.90 to 2.46 kPa

on the Philips platform. Mean liver stiffness values for the five clinical patients ranged from 2.1 to 4.94 kPa on the GE platform, and from 2.08 to 5.02 kPa on the Philips platform (Table 2). Liver stiffness differences ranged from 0.04 to 0.23 for the volunteer subjects and from 0.01 to 0.36 for the clinical patients. Cross-comparison of values for the 13 subjects across the two scanner platforms results in a highly reproducible measure of liver stiffness with an interclass correlation coefficient (ICC) value of 0.994 (95% confidence interval: 0.97–0.998), with  $p$  value  $<0.001$  indicating a significantly positive correlation. Figure 3A is a Bland–Altman plot displaying the mean differences in values for all 13 subjects falling within two standard deviations with the exception of one borderline outlier. Figure 3B shows a Scatter diagram between the two measurements, and all values fall within 95% prediction limits. Power analysis showed that while only 13 subjects were included in this pilot investigation, a power of 92% was still achieved to detect a correlation of 0.99 or higher assuming the null correlation at 0.85.

## Discussion

As MRE becomes more widespread in its availability and usage, and as more vendor platforms become approved for routine clinical by the FDA for determination of liver stiffness, it is imperative that cross-vendor validation studies be performed to ensure that liver stiffness values are consistent across different platforms. This consistency will ensure that surveillance exams can be performed on individual patients with chronic liver disease at different facilities, with different MR platforms, but without concern for variation in liver stiffness results secondary to purely technical factors.

While there have been several reports in the literature confirming the high reproducibility of MRE-derived liver stiffness values on the same subject performed at different time points, these studies were all performed on the same vendor platform [21, 22]. To our knowledge, there have been no reports in the literature demonstrating reproducibility of MRE-derived liver stiffness values on the same individual on different platforms. In this small pilot investigation, we have demonstrated that on two specific vendor platforms (GE and Philips). MRE-assessed liver stiffness is highly reproducible with an ICC for inter-platform agreement of 0.994 in this investigation. This reproducibility is a significant advantage of MRE compared to ultrasound elastography, in which there is a demonstrably lower rate of reproducibility in

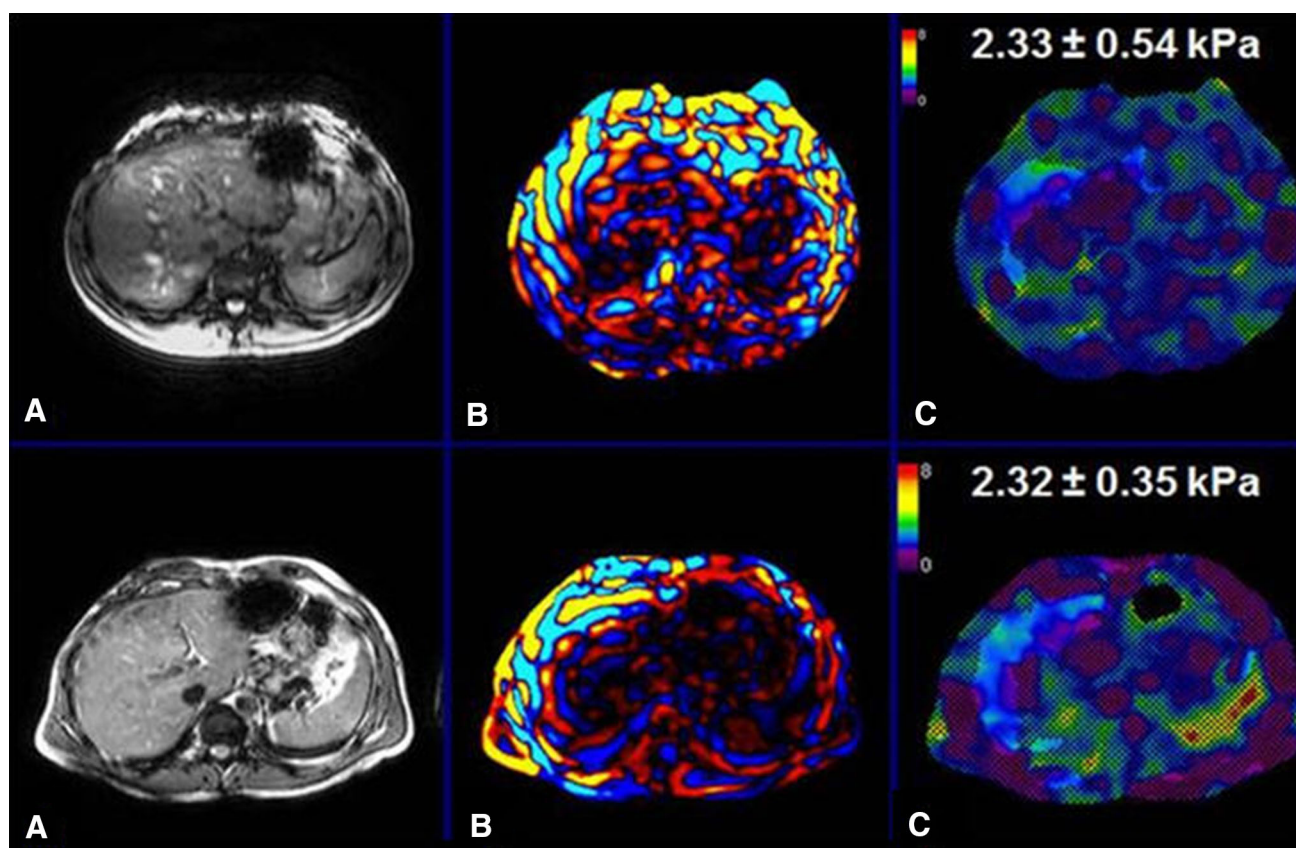


Fig. 2. Representative MRE images from the same subject performed on a GE MR scanner (*top row*) and a Philips MR scanner (*bottom row*): **A** magnitude images, **B** wave images, **C** color-coded MRE stiffness maps.

**Table 2.** MRE findings for 8 volunteers and 5 clinical patients acquired on both scanners

Subject/clinical patient	Liver stiffness (in kPa) on a GE magnet	Liver stiffness (in kPa) on a Philips magnet	Difference between values (absolute value in kPa)	Age (Years)	Sex (M/F)	Clinical indication
<b>Volunteer</b>						
1	2.13	1.96	0.17	38	F	
2	2.19	2.15	0.04	39	F	
3	2.02	1.96	0.06	34	F	
4	1.96	1.9	0.06	37	M	
5	2.12	1.96	0.16	32	F	
6	2.14	2.07	0.07	31	M	
7	2.65	2.46	0.19	55	M	
8	2.5	2.27	0.23	44	M	
<b>Patient</b>						
1	2.1	2.08	0.02	12	F	Nonalcoholic fatty liver disease
2	4.04	4.05	0.01	21	F	Fontan
3	3.91	3.55	0.36	17	F	Fontan
4	4.94	5.02	0.08	10	M	Wiskott–Aldrich syndrome
5	4.35	4.44	0.09	14	M	Fontan

liver stiffness values, both on the same equipment and when comparing values between different vendors/methods [23–25].

We do note a trend for the liver stiffness values on the Philips platform to run slightly lower than those on the GE platform. The exact etiology and clinical significance of this finding is uncertain at this point, but an area for

future investigation. We suspect that this finding may relate to the signal-to-noise properties of the MRE images on individual vendor MR scanners. Limitations of this study include its small sample size, relative small range of liver stiffness values in these thirteen individuals, lack of liver histopathology correlation to ascertain accuracy of the stiffness measurements relative to fibrosis

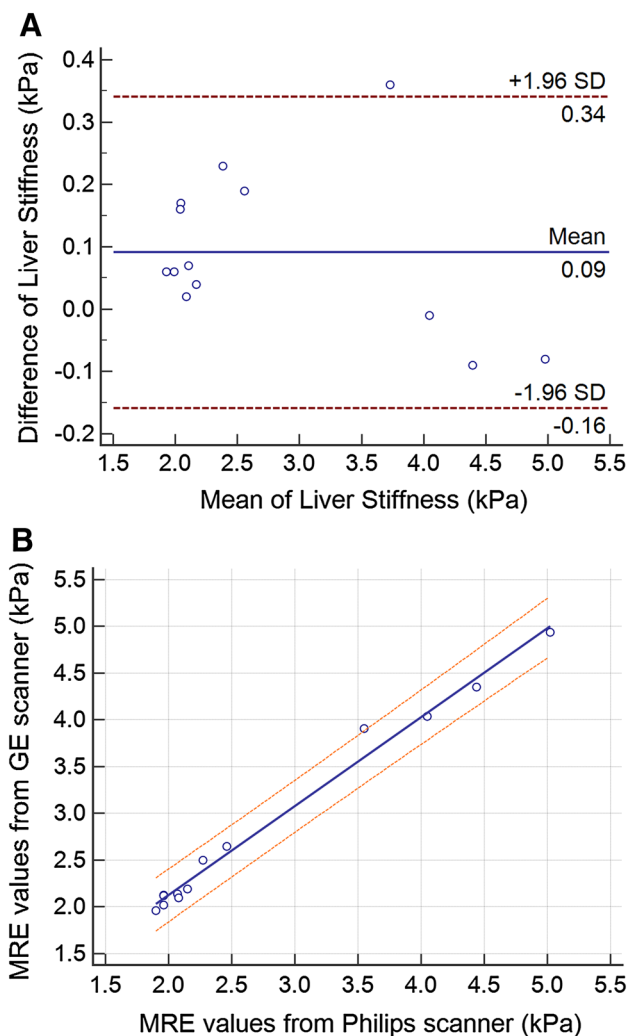


**Fig. 3.** **A** Bland–Altman plot showing mean difference values for all subjects fall within two standard deviations with the exception of one borderline outlier. **B** Scatter plot between both measurements showing all values fall within 95% prediction limits.

grade, and restriction to only two MR vendors at a single institution with MRE capability, both 1.5 T magnets. Differences between MRE-derived liver stiffness values between 1.5 and 3 T magnets were not evaluated in this study. Larger, multi-institutional studies in healthy volunteers and in clinical patients with chronic liver disease, to include other vendor platforms, will be needed to confirm reproducibility of these preliminary findings.

## Conclusion

Liver MRE is a promising non-invasive quantitative imaging tool used to determine liver stiffness in the assessment of patients with chronic liver disease. Because MRE visually quantifies and localizes the extent of tissue

stiffness throughout the liver, it provides the opportunity to create a visual map of the extent of fibrosis in the whole liver. In this small pilot investigation, we demonstrate that liver stiffness measurement with MRE is reproducible and has very good consistency across two vendor platforms. **Acknowledgements** Partial support from NIH grant EB001981 to RLE.

*Acknowledgements.* Partial support from NIH grant EB001981 to RLE.

*Conflict of interest.* RLE and the Mayo Clinic hold patents and have a financial interest through royalties related to MRE technology. HW is an employee of Philips Healthcare. DJP received travel reimbursement from Philips Healthcare.

## References

1. Beath SV (1994) Liver disorders in childhood. *Arch Dis Child* 71(4):390
2. Friedman SL (2003) Liver fibrosis—from bench to bedside. *J Hepatol* 38(Suppl 1):S38–S53
3. Friedman SL (2010) Evolving challenges in hepatic fibrosis. *Nat Rev Gastroenterol Hepatol* 7(8):425–436. doi:10.1038/nrgastro.2010.97
4. Mieli-Vergani G, Vergani D (2008) Autoimmune paediatric liver disease. *World J Gastroenterol* 14(21):3360–3367
5. Brunt EM (2010) Pathology of nonalcoholic fatty liver disease. *Nat Rev Gastroenterol Hepatol* 7(4):195–203. doi:10.1038/nrgastro.2010.21
6. Bortolotti F, Guido M (2007) Reversal of liver cirrhosis: a desirable clinical outcome and its pathogenic background. *J pediatr Gastroenterol Nutr* 44(4):401–406. doi:10.1097/MPG.0b013e318032069a
7. Naini BV, Lassman CR (2012) Total parenteral nutrition therapy and liver injury: a histopathologic study with clinical correlation. *Hum Pathol* 43(6):826–833. doi:10.1016/j.humpath.2011.07.008
8. Castera L, Pinzani M (2010) Biopsy and non-invasive methods for the diagnosis of liver fibrosis: does it take two to tango? *Gut* 59(7):861–866. doi:10.1136/gut.2010.214650
9. Pariente D, Franchi-Abella S (2010) Paediatric chronic liver diseases: how to investigate and follow up? Role of imaging in the diagnosis of fibrosis. *Pediatr Radiol* 40(6):906–919. doi:10.1007/s00247-010-1600-3
10. Straub BK, Schirmacher P (2010) Pathology and biopsy assessment of non-alcoholic fatty liver disease. *Dig Dis* 28(1):197–202. doi:10.1159/000282086
11. Regev A, Berho M, Jeffers LJ, et al. (2002) Sampling error and intraobserver variation in liver biopsy in patients with chronic HCV infection. *Am J Gastroenterol* 97(10):2614–2618. doi:10.1111/j.1572-0241.2002.06038.x
12. Xanthakos SA, Podberesky DJ, Serai SD, et al. (2014) Use of magnetic resonance elastography to assess hepatic fibrosis in children with chronic liver disease. *J Pediatr* 164(1):186–188. doi:10.1016/j.jpeds.2013.07.050
13. Yin M, Talwalkar JA, Glaser KJ, Manduca A, Grimm RC, Rossman PJ, Fidler JL, Ehman RL (2007) Assessment of hepatic fibrosis with magnetic resonance elastography. *Clin Gastroenterol Hepatol* 5 (10):1207–1213.e1202. doi:10.1016/j.cgh.2007.06.012
14. Serai SD, Towbin AJ, Podberesky DJ (2012) Pediatric liver MR elastography. *Dig Dis Sci* 57(10):2713–2719. doi:10.1007/s10620-012-2196-2
15. Serai SD, Wallihan DB, Venkatesh SK, et al. (2014) Magnetic resonance elastography of the liver in patients status-post fontan procedure: feasibility and preliminary results. *Congenit Heart Dis* 9(1):7–14. doi:10.1111/chd.12144
16. Towbin AJ, Serai SD, Podberesky DJ (2013) Magnetic resonance imaging of the pediatric liver: imaging of steatosis, iron deposition, and fibrosis. *Magn Reson Imaging Clin North Am* 21(4):669–680. doi:10.1016/j.mric.2013.05.001
17. Wallihan DB, Podberesky DJ, Marino BS, Sticka JS, Serai S (2013) Relationship of MR elastography determined liver stiffness with cardiac function after Fontan palliation. *J Magn Reson Imaging* . doi:10.1002/jmri.24496

18. Manduca A, Oliphant TE, Dresner MA, et al. (2001) Magnetic resonance elastography: non-invasive mapping of tissue elasticity. *Med Image Anal* 5(4):237–254
19. Bland JM, Altman DG (1986) Statistical methods for assessing agreement between two methods of clinical measurement. *Lancet* 1(8476):307–310
20. Bland JM, Altman DG (2012) Agreed statistics: measurement method comparison. *Anesthesiology* 116(1):182–185. doi:[10.1097/ALN.0b013e31823d7784](https://doi.org/10.1097/ALN.0b013e31823d7784)
21. Lee Y, Lee JM, Lee JE, et al. (2014) MR elastography for noninvasive assessment of hepatic fibrosis: reproducibility of the examination and reproducibility and repeatability of the liver stiffness value measurement. *J Magn Reson Imaging* 39(2):326–331. doi:[10.1002/jmri.24147](https://doi.org/10.1002/jmri.24147)
22. Shi Y, Glaser KJ, Venkatesh SK, Ben-Abraham EI, Ehman RL (2014) Feasibility of using 3D MR elastography to determine pancreatic stiffness in healthy volunteers. *J Magn Reson Imaging* . doi:[10.1002/jmri.24572](https://doi.org/10.1002/jmri.24572)
23. Bota S, Sporea I, Sirli R, et al. (2012) Intra- and interoperator reproducibility of acoustic radiation force impulse (ARFI) elastography—preliminary results. *Ultrasound Med Biol* 38(7):1103–1108. doi:[10.1016/j.ultrasmedbio.2012.02.032](https://doi.org/10.1016/j.ultrasmedbio.2012.02.032)
24. Ebinuma H, Saito H, Komuta M, et al. (2011) Evaluation of liver fibrosis by transient elastography using acoustic radiation force impulse: comparison with Fibroscan((R)). *J Gastroenterol* 46(10):1238–1248. doi:[10.1007/s00535-011-0437-3](https://doi.org/10.1007/s00535-011-0437-3)
25. Rizzo L, Calvaruso V, Cacopardo B, et al. (2011) Comparison of transient elastography and acoustic radiation force impulse for non-invasive staging of liver fibrosis in patients with chronic hepatitis C. *Am J Gastroenterol* 106(12):2112–2120. doi:[10.1038/ajg.2011.341](https://doi.org/10.1038/ajg.2011.341)